Structure, Stability, Thermodynamic Properties, and Infrared Spectra of the Protonated Water Octamer $H^+(H_2O)_8$

S. Karthikeyan, Mina Park, Ilgyou Shin, and Kwang S. Kim*

Center for Superfunctional Materials, Department of Chemistry, Pohang University of Science and Technology, San 31, Hyojadong, Namgu, Pohang 790-784, Korea

Received: May 31, 2008; Revised Manuscript Received: July 17, 2008

We investigated various two-dimensional (2D) and three-dimensional (3D) structures of $H^+(H_2O)_8$, using density functional theory (DFT), Moller−Plesset second-order perturbation theory (MP2), and coupled cluster theory with single, double, and perturbative triple excitations (CCSD(T)). The 3D structure is more stable than the 2D structure at all levels of theory on the Born−Oppenheimer surface. With the zero-point energy (ZPE) correction, the predicted structure varies depending on the level of theory. The DFT employing Becke's three parameters with Lee−Yang−Parr functionals (B3LYP) favors the 2D structure. At the complete basis set (CBS) limit, the MP2 calculation favors the 3D structure by 0.29 kcal/mol, and the CCSD(T) calculation favors the 3D structure by 0.27 kcal/mol. It is thus expected that both 2D and 3D structures are nearly isoenergetic near 0 K. At 100 K, all the calculations show that the 2D structure is much more stable in free binding energy than the 3D structure. The DFT and MP2 vibrational spectra of the 2D structure are consistent with the experimental spectra. First-principles Car−Parrinello molecular dynamics (CPMD) simulations show that the 2D Zundel-type vibrational spectra are in good agreement with the experiment.

Introduction

The study of protonated water clusters $H^+(H_2O)_n$ has been an important subject to understand the dissociation phenomena in aqueous chemistry and the transport phenomena in biological systems. In the protonated water clusters,[1−3] the proton can be either an Eigen form[4] (where the proton is bound to a single water molecule, forming H_3O^+) or a Zundel form[5] (where the proton is shared between two water molecules, forming $H_2O\cdots H^+\cdots OH_2$). This has raised the question of which form would be more stable for the given n. Theoretical studies of structures of hydrated proton have been carried out from empirical potentials[6,7] to ab initio calculations.[8−10] A number of studies on the structural changes of the protonated water clusters with increasing cluster size have also been reported,[1,7,9b] because these structures are quite different from those of neutral water clusters,[11−13] anionic water clusters,[14,15] and water clusters containing a cation.[16] In the case of the neutral water octamer, the three-dimensional (3D) cubical structure is particularly stable.[11b,12g,13e] Though the hydrogen orientations are different, even the lowest energy structure of the anionic water octamer or the water octamer binding an excess electron $[e^- + (H_2O)_8]$ has the cubic skeleton.[15a,c] Therefore, one might expect that the protonated water octamer could have the cubical skeleton. Nevertheless, the experimental spectra seem to be against this structure. It is thus still unknown at what size (n) of $H^+(H_2O)_n$ the two-dimensional (2D) to 3D transition takes place.

Although there was a controversial issue over the 2D versus 3D structure even for $n = 7$, it is now known that even at 0 K, the 2D structure is more stable than the 3D structure.[10] Then, the controversial issue over the 2D versus 3D structure for $n = 8$ (protonated water octamer) needs to be resolved, because this cluster has been differently proposed as a 2D cyclic,[1,3] 2D noncyclic,[2b] or 3D[7] structure. Jiang et al. proposed a 2D structure based on the comparison of the density functional theory (DFT) calculated IR spectra with the experimentally observed IR spectra (though not based on the energies).[3] The empirical Kozack−Jordan (KJ) model potential of H_3O^+ predicted a 3D structure as the lowest energy structure.[7] Recently, the IR spectra of $H^+(H_2O)_8$ were further investigated by a few groups; Headrick et al.[1] and Miyazaki et al.[2b] proposed a 2D net-type structure. In this regard, a more accurate theoretical investigation is required. We have carried out DFT, MP2, and CCSD(T) calculations. To find a more accurate conclusion, we have focused our attention to the following: (a) interaction energy at high levels of theory; (b) zero-point energy (ZPE) correction; (c) complete basis set (CBS) limit; (d) comparison of the DFT and Moller−Plesset second-order perturbation theory (MP2) predicted spectra with the experimental spectra;[1] (e) comparison of the Car−Parrinello molecular dynamics (CPMD) spectra with the experimental spectra.[1]

Computational Methods

To find the lowest energy structure, we carried out the basin-hopping global optimization[17] using the density functional based tight-binding (DFTB) method.[18] By using the Gaussian 03 suite of programs,[19] the low-energy structures were optimized and the harmonic frequencies were obtained at the DFT level using the Becke three parameters with the Lee−Yang−Parr functional[20] (B3LYP) and the MP2 level of theory for which the aug-cc-pVDZ (abbreviated as aVDZ) basis set was employed. The MP2/aug-cc-pVTZ (abbreviated as aVTZ) and CCSD(T)/aVDZ energies were obtained using the single-point energy calculations on the MP2/aVDZ geometries. We estimated the MP2/CBS binding energies using the extrapolation scheme which utilizes that the electron correlation is proportional to N^{-3} for aug-cc-pVNZ basis sets.[21,22] The CCSD(T)/CBS energies were estimated by assuming that the difference in binding energies between MP2/aVDZ and MP2/CBS calculations is similar to that between CCSD(T)/aVDZ and CCSD(T)/CBS calculations.[22,23] The molecular structures were drawn with the

* Corresponding author. E-mail: kim@postech.ac.kr.

10.1021/jp804806u CCC: $40.75
Published on Web 09/13/2008

POSMOL package.[24] We have investigated the spectral features of $H^+(H_2O)_8$ at the B3LYP/aVDZ and MP2/aVDZ levels of theory. The scale factor 0.970/0.959 at the B3LYP/MP2 level of theory was chosen from the comparison of the experimental and calculated average values of asymmetric and symmetric OH stretching frequencies of the water monomer.[25]

For first-principles CPMD simulations, we employed the DFT method with the Becke−Lee−Yang−Parr (BLYP) functionals. These CPMD simulations were carried out for 10 ps at 100 K by using the CPMD code.[26] The core−valence interaction was described by a norm-conserving Trouiller−Martins pseudopotential.[27] Valence wave functions were expanded in a plane wave basis set with an energy cutoff value of 90 Ry. A fictitious electron mass of 600 au and an integration step of $\Delta t = 4.135$ au (0.1 fs) were used.[28] A Nose−Hoover thermostat[29] was attached to every degree of freedom to ensure proper thermalization over the CPMD trajectory. During the simulations, we kept the molecules at the center of isolated cubic boxes of side lengths $L = 10$ Å. From the last 6 ps trajectory of each CPMD simulation, we evaluated the time correlation function to investigate the spectra of the clusters in the equilibrium state. The Fourier transform of dipole moment autocorrelation functions (FT-DACF) was carried out.

The IR absorption spectrum can be computed from FT-DACF as

$$I(\omega) = (\hbar\beta/2\pi)\omega^2 \int dt\, e^{-i\omega t}\langle\mu(0)\mu(t)\rangle$$

Here, the symbols are used to denote intensity (I), frequency (ω), Plank constant ($\hbar = h/2\pi$), inverse of Boltzmann constant multiplied by temperature ($\beta = 1/kT$), time (t), and dipole moment (μ). For computational and interpretative purposes, it is, however, more convenient to compute the autocorrelation function of the time derivative of the dipole moment:

$$I(\omega) = \frac{\hbar\beta}{2\pi} \int dt\, e^{-i\omega t}\langle\dot{\mu}(0)\dot{\mu}(t)\rangle$$

as discussed by Schmitt and Voth.[30] Therefore, this method was employed in our calculations. Since FT-DACF provides the information about dipole moment change due to vibrational motions, the result is in general similar to the experimental IR spectrum. The Fourier transform of velocity autocorrelation function (FT-VACF) is often useful for the frequency analysis along with intensities representing the rovibrational density of states. This FT-VACF was used in our mode analysis to find how a specific stretching/bending mode is associated with what kind of atomic motions. The vibrational frequencies for FT-DACF and FT-VACF of the CPMD simulations at 100 K were scaled with the factor of 1.049, as in our previous work.[8e,31]

The FT-DACF is known to be more realistic. However, the intensity of the spectra in a high-frequency region (>3500 cm^{-1}) often tends to be poorly described (i.e., underestimated), and so the peaks are too weak (or almost disappear).[8e,9d,31] On the other hand, the FT-VACF, which also reflects some of the power spectra, often overestimates the intensity of the spectra in a high-frequency region.

Results and Discussion

Since there are many low-energy structures for the protonated water octamer $[H^+(H_2O)_8]$ cluster, we searched for the candidates for the lowest energy structure with the basin-hopping global optimization using the DFTB method.[18] Then, important low-energy structures were further selected based on the B3LYP/aVDZ energies. Previously reported structures[1,3,6,7] were also considered for comparison. Five important low-energy structures (whereas others are at least 2−3 kcal/mol higher in energy than the lowest one at the MP2/aVDZ level) are given in Figure 1, where 2D/3D denotes two/three-dimensional structure and the numbers "n_1n_2..." after "D" denote the n_1-, n_2-,... membered rings. Each hydrogen atom of the H_3O^+ ion involves a hydrogen bond as a strong hydrophilic site, whereas the oxygen atom of the H_3O^+ ion behaves as a hydrophobic site due to the three positively charged hydrogen atoms that hinder the close approach toward the oxygen center from other hydrogen atoms. The H_3O^+ ion tends to be on the surface of the cluster, and the three hydrogen atoms of the H_3O^+ ion are bonded by three water molecules. Thus, the H_3O^+ ion favors the trihydrogen-bonded structure.

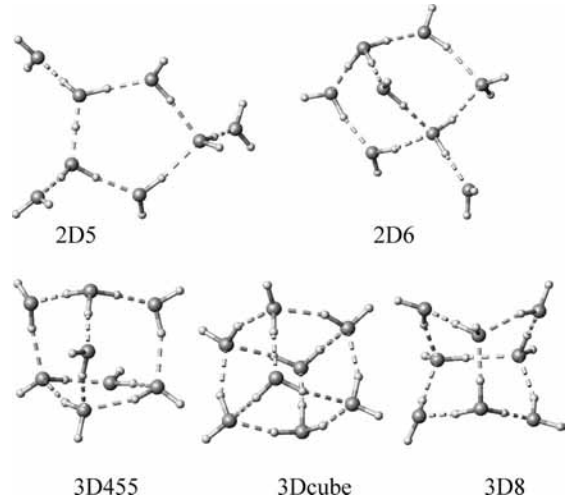

Figure 1. Low-energy structures of the $H^+(H_2O)_8$ cluster.

TABLE 1: B3LYP/aVDZ Binding Energies and Thermodynamic Quantities (kcal/mol) for Low-Energy Structures of $H^+(H_2O)_8$[a]

	B3LYP/aVDZ			
	$-\Delta E_e$	$-\Delta E_0$	$-\Delta H$(298 K)	$-\Delta G$(298 K)
2D5	127.22	**113.81**	**98.55**	**59.95**
2D6	**128.73**	111.75	98.17	53.10
3D455	**130.74**	**112.97**	**100.06**	**52.69**
3Dcube	127.74	108.98	96.80	47.09
3D8	129.70	111.94	99.20	51.28

[a] The lowest energies for 2D and 3D structures are marked in bold.

The predicted binding energies and thermodynamic quantities of all isomers at the B3LYP/aVDZ level are in Table 1. Among these structures, the 2D Zundel structure (2D5) is the most stable at the B3LYP/aVDZ level, whereas the empirical KJ (H_3O^+) model potential favors the 3D Eigen structure[7] (3D455). At the B3LYP/aVDZ level, the 2D Zundel ion (2D5) is less stable than the 3D Eigen ion (3D455) by 3.52 kcal/mol in ZPE-uncorrected binding energy ($-\Delta E_e$) but more stable by 0.84 kcal/mol in ZPE-corrected binding energy ($-\Delta E_0$) and by 7.26 kcal/mol in free binding energy ($-\Delta G$(298 K)).

Thus, we have further investigated them at higher levels of theory. The binding energies and thermodynamic quantities of the isomers at the MP2/aVDZ, MP2/aVTZ, MP2/CBS, CCSD(T)/aVDZ, and CCSD(T)/CBS levels are given in Table 2. At the MP2/CBS and CCSD(T)/CBS levels, the 3D455 isomer is predicted to be the most stable isomer in ZPE-uncorrected/corrected interaction energy ($\Delta E_e/\Delta E_0$). In ΔE_e, the 3D conformer (3D455) is more stable than the 2D conformer (2D5)

TABLE 2: MP2 and CCSD(T) Binding Energies and Thermodynamic Quantities (kcal/mol) for Low-Energy Structures of $H^+(H_2O)_8$[a]

	$-\Delta E_e$	$-\Delta E_0$	$-\Delta H$(100 K)	$-\Delta G$(100 K)
		MP2/aVDZ		
2D5	119.01	**104.94**	**108.42**	**89.52**
2D6	**119.49**	103.14	106.97	87.07
3D455	**122.89**	**104.82**	**109.07**	**88.22**
3D8	121.80	103.71	107.98	87.06
		MP2/aVTZ		
2D5	124.18	**110.11**	**113.58**	**94.68**
2D6	**124.56**	108.21	112.05	92.15
3D455	**128.34**	**110.27**	**114.52**	**93.66**
3D8	127.39	109.31	113.58	92.65
		MP2/CBS		
2D5	126.35	**112.28**	**115.76**	**96.86**
2D6	**126.70**	110.35	114.19	94.28
3D455	**130.63**	**112.57**	**116.81**	**95.96**
3D8	129.75	111.66	115.94	95.01
		CCSD(T)/aVDZ		
2D5	117.32	**103.25**	**106.73**	**87.83**
2D6	**117.90**	101.55	105.39	85.49
3D455	**121.18**	**103.12**	**107.36**	**86.51**
3D8	120.04	101.96	106.23	85.30
		CCSD(T)/CBS		
2D5	124.66	**110.59**	**114.07**	**95.17**
2D6	**125.11**	108.76	112.60	92.70
3D455	**128.93**	**110.86**	**115.11**	**94.25**
3D8	128.00	109.91	114.19	93.26

[a] The BSSE corrections were made. CCSD(T)/CBS energies were estimated by applying the correction term (the difference between MP2/aVDZ and CCSD(T)/aVDZ energies) to the MP2/CBS interaction energies which were obtained with the extrapolation scheme utilizing the electron correlation proportional to N^{-3} for the aug-cc-pV*N*Z basis set. The lowest energies for 2D and 3D structures are marked in bold.

by 4.28 kcal/mol at the MP2/CBS level and 4.27 kcal/mol at the CCSD(T)/CBS level. The ZPE correction reduces such stability drastically, so at 0 K, the ZPE-corrected 2D5 and 3D455 isomers are nearly isoenergetic. Namely, in ΔE_0, the 3D conformer (3D455) is only slightly more stable than the 2D conformer (2D5) by 0.29 kcal/mol at the MP2/CBS level and 0.27 kcal/mol at the CCSD(T)/CBS level. However, in free energy (ΔG(100 K)), 2D5 is more stable than 3D455 by 0.91 kcal/mol at the CCSD(T)/CBS level and by 0.92 kcal/mol at the MP2/CBS level. This stability change among isomers depending on temperature can be more clearly seen from the plot (Figure 2) of their relative values in ZPE-uncorrected energy (ΔE_e), ZPE-corrected energy (ΔE_0), and free energies (ΔG(50 K), ΔG(100 K), ΔG(150 K), ΔG(200 K)) at the CCSD(T)/CBS level. At 0 K, the 3D structure (3D455) would be the most stable (though nearly isoenergetic to the 2D structure (2D5)); around 40 K, the 2D structure (2D5) becomes the most stable; around 150 K the 3D structure (3D455) is less stable than even the second lowest 2D structure (2D6).

In protonated water clusters, the individual water monomer is linked by different kinds of H-bonds such as single-proton acceptor (A), single acceptor−single donor (AD), single acceptor−double donor (ADD), double acceptor−single donor (AAD), and double acceptor−double donor (AADD). The spectral shifts are found to be strongly dependent on the number of donors, whereas their dependency on the number of acceptors is rather small.[32] Each type of molecule in the clusters tends to show its own characteristic frequency shifts depending on its H-bond type. Many previous vibrational frequencies reported

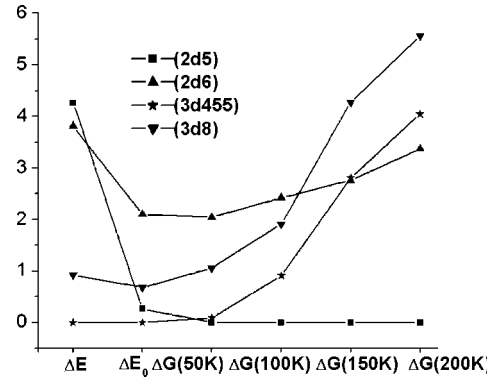

Figure 2. Relative stability (in ΔE_e, ΔE_0, ΔG(50 K), ΔG(100 K), ΔG(150 K), and ΔG(200 K)) of the low-lying energy isomers of $H^+(H_2O)_8$ at the CCSD(T)/CBS levels of theory.

by experiments are mostly based on the OH stretching modes of the water molecule, whereas few experiments reported the motion of the proton which interconverts between the Eigen- and Zundel-type ion cluster.[1−3] The vibrations associated with the excess proton in these clusters occur at much lower frequencies than the general OH stretching frequencies. Thus, we also considered the spectral region below the OH vibrational stretching frequencies. Table 3 reports B3LYP/aVDZ frequencies, MP2/aVDZ frequencies, and CPMD frequencies, which are compared with the available experimental frequencies.[1]

In Figure 3, we have shown the B3LYP/aVDZ, MP2/aVDZ vibrational spectra, FT-DACF, and FT-VACF power spectra for the 2D5 and 3D455 structures along with the experimental vibrational spectra. The B3LYP/aVDZ spectra are overall in good agreement with the experimental spectra, although the detailed frequency values are somewhat deviated. Our frequency analysis vis-à-vis the experimental data will be on the basis of the CPMD power spectra at 100 K which show better agreements with experiments than the scaled harmonic vibrational frequencies of B3LYP and MP2 spectra at 0 K. Experimentally reported vibrational spectra of the protonated water octamer [$H^+(H_2O)_8$] cluster indicate that $H^+(H_2O)_8$ has the Zundel-type structure.[1] However, it should be recalled that the 2D Zundel-type (2D5) and 3D Eigen-type (3D455) structures are nearly isoenergetic at 0 K, whereas the 2D5 is much more stable than 3D455 at 100 K. According to the ΔG value at 100 K, the 2D5 isomer is ∼90 times more abundant than the 3D455 isomer, which indicates that if the experimental spectra were observed around 100 K, they should reflect the spectra of 2D5.

The predicted CPMD power spectra of the 2D Zundel-type (2D5) and the 3D Eigen-type (3D455) are similar to the experimental spectrum in the range of 3350−3800 cm^{-1} but are different in the lower vibrational spectra. The power spectra of the 2D Zundel structure (2D5) look similar to the experimental vibrational spectra, whereas that of the 3D Eigen structure (3D455) is not. Thus, we conclude that the structure of the $H^+(H_2O)_8$ cluster observed in the experiment (probably carried out more than 100 K) was the Zundel form.

We also note that the OH stretching frequencies appear in the region of 2900−3800 cm^{-1}. The predicted vibrational stretching frequencies for the symmetric (ν_s AH_d) and asymmetric (ν_a AH_d) dangling hydrogen of water appear around 3652 (B3LYP, 3679−3682; MP2, 3637−3641) and 3750 (B3LYP, 3780−3783; MP2, 3755−3761) cm^{-1}, respectively, which are in good agreement with the experimentally observed vibrational frequencies of 3650 and 3740 cm^{-1}. However, the 3D Eigen-type (3D455) conformer does not have the AH_d-type vibrational

TABLE 3: Vibrational Frequencies of $H^+(H_2O)_8$ Predicted by B3LYP/aVDZ (Scale Factor, 0.970), MP2/aVDZ (Scale Factor, 0.959), CPMD Simulation (Scale Factor, 1.049), and the Experimental Frequencies (Ref 1)[a]

	B3LYP/aVDZ		MP2/aVDZ		CPMD		
mode	2D5	3D455	2D5	3D455	2D5	3D455	exptl[b]
ν_a AH_d	3783_w, 3780_w		3761_w, 3759_w, 3755_w		3750_w		**3740_m**
ν_a ADH_d	3751_w, 3745_w	3753_w, 3746_w, 3741_w, 3738_w	3724_w, 3715_w	3729_w, 3713_w, 3710_w, 3704_w	**3719_m**	**3720_m**	**3715_m**
ν_s $AADH_d$	3717_w	3720_w, 3716_w, 3713_w	3690_w	3692_w, 3683_w, 3680_w	**3692_m**	**3689_m**	**3685_m**
ν_s AH_d	3682_w, 3680_w, 3679_w		3641_w, 3640_w, 3637_w		3652_w		3650_w
ν ADH_h	**3471_m**, **3402_m**	**3535_m**, **3455_m**, **3422_m**, **3392_m**, **3381_m**	**3472_m**, **3395_m**	3528_w, 3449_w, **3417_m**, 3391_w, **3378_m**	**3451_m**, **3419_m**	**3434_m**, **3402_s**	**$\sim3430_m$**
ν $AADH_h$	**3321_s**	**3303_m**, **3162_m**	**3329_s**	**3310_m**, **3192_m**	**3330_m**	3028_w	**$\sim3365_s$**
ν_s H_3O^+		**2840_m**		**2824_m**		**2748_s**	
ν_a H_3O^+		**2663_s**, **2630_s**		**2691_s**, **2660_s**		**2654_m**, **2582_m**	
ν H_3O^+ bend		1310_w		1322_w		**1329_m**	
ν Zundel ion	**3334_m**, **3211_m**, **3193_s**, **2993_s**		**3359_s**, **3244_m**, **3170_s**, **2954_s**		**3264_m**, **3144_m**, **3073_s**		**$\sim3200_m$**
ν Zundel bend	**1688_m**, **1679_m**, 1345_w, **1104_s**, 982_w		**1711_s**, 1693_w, **1372_s**, **1304_s**, 1019_w		**1642_m**, **1085_m**		**1650_m**, **1055_s**

[a] ν, stretching mode; ν_s/ν_a, symmetric/asymmetric stretching modes; H_d, dangling hydrogen seen in A, AD, and AAD types of hydrogen bonding of H_2O; H_h, hydrogen-bonded hydrogen. IR intensities are denoted in subscripts (s, strong; m, medium; w, weak). The medium and strong peaks are marked in bold. The predicted peaks are marked with underline when their intensity is in reasonable agreement with the experimental intensity. [b] Ref 1.

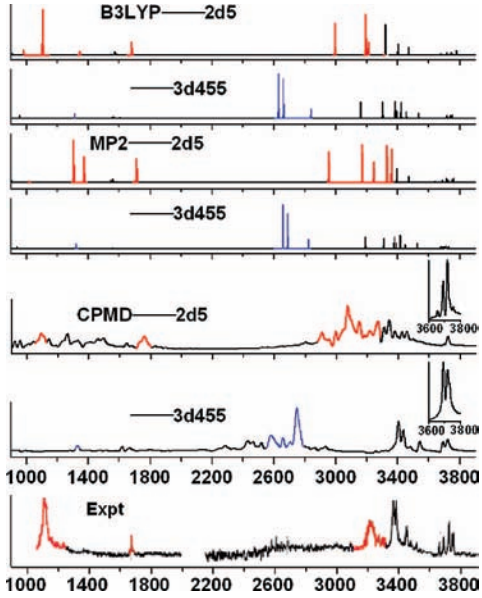

Figure 3. B3LYP/aVDZ (with a scale factor of 0.970), MP2/aVDZ (with a scale factor of 0.959), and CPMD (with a scale factor of 1.049) predicted vibrational spectra of the 2D5 and 3D455 conformers of the $H^+(H_2O)_8$ cluster and the experimental spectra (ref 1). Eigen peaks are highlighted in blue color, and Zundel peaks are highlighted in red color. The CPMD power spectra are drawn in FT-DACF, while each inset for the frequencies around ~3700 cm^{-1} is given in FT-VACF.

stretching frequencies. The predicted CPMD vibrational spectra of the dangling hydrogen (ν ADH_d) appear at 3719 (2D5) and 3720 cm^{-1} (3D455), consistent with the experimental frequency at 3715 cm^{-1}. Hydrogen-bonded OH stretching frequencies (ν ADH_d) appear at 3451, 3419 cm^{-1} for the 2D5 conformer and 3434, 3402 cm^{-1} for the 3D455 conformer, which are close to the experimental peaks around 3400 cm^{-1}. These peaks are red-shifted due to the excess proton. The predicted vibrational stretching frequencies of the dangling hydrogen of water (ν $AADH_d$) appear at 3692 cm^{-1} for the 2D5 conformer and 3689 cm^{-1} for the 3D455 conformer, close to the experimentally observed vibrational frequencies of the dangling hydrogen of water (ν $AADH_d$) at 3685 cm^{-1}.

The CPMD frequencies of asymmetric (ν_s H_3O^+), symmetric (ν_s H_3O^+), and bending modes of H_3O^+ ions (ν_b H_3O^+) for 3D455 are predicted to appear at 3028, 2748, and 1329 cm^{-1}, respectively. However, no such kind of peak appears in the experimental vibrational spectra. The CPMD predicted power spectrum of 2D5 shows a strong peak at 1085 cm^{-1} and a peak at 1642 cm^{-1}, which correspond to the experimentally observed strong oscillation of the shared proton in the Zundel-type ion (1055 cm^{-1}) and the experimental peak corresponding to the bending of water in the Zundel ion (1650 cm^{-1}), respectively. The CPMD predicted asymmetric stretching vibrational frequencies of the Zundel ion appear at 3073, 3144, 3264 cm^{-1} (B3LYP, 2993, 3193, 3211, 3334 cm^{-1}; MP2, 2954, 3170, 3244, 3359 cm^{-1}), consistent with the experimental peak around 3200 cm^{-1}. We particularly note that the CPMD simulated vibrational spectra of the 2D5 structure are in good agreement with the experimental spectra, as shown in Table 3 and Figure 3. On the other hand, the CPMD power spectra of the 3D455 structure do not agree with the experimental[1] spectra, as noted from Table 3 and Figure 3.

Conclusion

We have studied the structural isomer, stability, thermodynamic properties, and IR spectra of the protonated water cluster of $H^+(H_2O)_8$. The controversial issue regarding the structure of the $H^+(H_2O)_8$ clusters is resolved. The B3LYP/aVDZ calculations show that the 3D455 structure is the most stable on the Born−Oppenheimer potential surface (i.e., in the ZPE-uncorrected interaction energy, ΔE_e). However, after the ZPE correction, the 2D5 structure is the most stable at the B3LYP/aVDZ levels of theory, but at the MP2/CBS and CCSD(T)/CBS levels, the 2D5 is slightly more stable than the 3D455 (though they are nearly isoenergetic). At 100 K, the 2D5 is much more stable (in free energy) than 3D455, indicating that the

2D5 structure would have been observed in experiments carried out around 100−200 K. CPMD simulated power spectra of the 2D5 conformer are overall in good agreement with the experimental spectra of $H^+(H_2O)_8$.[1]

Acknowledgment. This work was supported by the Brain Korea 21 program and the GRL (KICOS) project. Calculations were carried out using supercomputers at KISTI (Grant No. KSC-2008-K08-0002).

References and Notes

(1) Headrick, J. M.; Diken, E. G.; Walters, R. S.; Hammer, N. I.; Christie, R. A.; Cui, J.; Myshakin, E. M.; Duncan, M. A.; Johnson, M. A.; Jordan, K. D. *Science* **2005**, *308*, 1765.

(2) (a) Asmis, K. R.; Pivonka, N. L.; Santambrogio, G.; Brummer, M.; Kaposta, C.; Neumark, D. M.; Wöste, L. *Science* **2003**, *299*, 1375. (b) Miyazaki, M.; Fujii, A.; Ebata, T.; Mikami, N. *Science* **2004**, *304*, 1134. (c) Shin, J.-W.; Hammer, N. I.; Diken, E. G.; Johnson, M. A.; Walters, R. S.; Jaeger, T. D.; Duncan, M. A.; Christie, R. A.; Jordan, K. D. *Science* **2004**, *304*, 1137. (d) Wu, C. C.; Lin, C. K.; Chang, H. C.; Jiang, J. C.; Kuo, J. L.; Klein, M. L. *J. Chem. Phys.* **2005**, *122*, 074315.

(3) Jiang, J. C.; Wang, Y. S.; Chang, H. C.; Lin, S. H.; Lee, Y. T.; Niedner-Schatteburg, G.; Chang, H. C. *J. Am. Chem. Soc.* **2000**, *122*, 1398.

(4) Eigen, M.; Maeyer, L. D. *Proc. R. Soc. London, Ser. A* **1958**, *247*, 505.

(5) Zundel, G.; Metzer, H. *Z. Phys. Chem. (Munich)* **1968**, *58*, 225.

(6) (a) Ojamäe, L.; Shavitt, I.; Singer, S. J. *J. Chem. Phys.* **1998**, *109*, 5547. (b) Kozack, R. E.; Jordan, P. C. *J. Chem. Phys.* **1992**, *96*, 3131.

(7) (a) Hodges, M. P.; Wales, D. J. *Chem. Phys. Lett.* **2000**, *324*, 279. (b) James, T.; Wales, D. J. *J. Chem. Phys.* **2005**, *122*, 134306.

(8) (a) Xie, Y.; Remington, R. B.; Schaefer, H. F., III *J. Chem. Phys.* **1994**, *101*, 4878. (b) Valeev, E. F.; Schaefer, H. F., III *J. Chem. Phys.* **1998**, *108*, 7197. (c) Wei, D.; Salahub, D. R. *J. Chem. Phys.* **1997**, *106*, 6086. (d) Kuo, J.-L.; Klein, M. L. *J. Chem. Phys.* **2005**, *122*, 024516. (e) Singh, N. J.; Park, M.; Min, S. K.; Suh, S. B.; Kim, K. S. *Angew. Chem., Int. Ed.* **2006**, *45*, 3795.

(9) (a) Park, M.; Shin, I.; Singh, N. J.; Kim, K. S. *J. Phys. Chem. A* **2007**, *111*, 10692. (b) Lee, H. M.; Tarakeshwar, P.; Park, J. W.; Kolaski, M. R.; Yoon, Y. J.; Yi, H.-B.; Kim, W. Y.; Kim, K. S. *J. Phys. Chem. A* **2004**, *108*, 2949. (c) Iyengar, S. S.; Petersen, M. K.; Day, T. J. F.; Burnham, C. J.; Teige, V. E.; Voth, G. A. *J. Chem. Phys.* **2005**, *123*, 084309. (d) Christie, R. A.; Jordan, K. D. *J. Phys. Chem. A* **2002**, *106*, 8376.

(10) Shin, I.; Park, M.; Min, S. K.; Lee, E. C.; Suh, S. B.; Kim, K. S. *J. Chem. Phys.* **2006**, *125*, 234305.

(11) (a) Pribble, R. N.; Zwier, T. S. *Science* **1994**, *265*, 75. (b) Gruenloh, C. J.; Carney, J. R.; Arrington, C. A.; Zwier, T. S.; Fredericks, S. Y.; Jordan, K. D. *Science* **1997**, *276*, 1678. (c) Buck, U.; Ettischer, I.; Melzer, M.; Buch, V.; Sadlej, J. J. *Phys. Rev. Lett.* **1998**, *80*, 2578.

(12) (a) Kim, K. S.; Dupuis, M.; Lie, G. C.; Clementi, E. *Chem. Phys. Lett.* **1986**, *131*, 451. (b) Mhin, B.-J.; Kim, H. S.; Kim, H. S.; Yoon, J. W.; Kim, K. S. *Chem. Phys. Lett.* **1991**, *176*, 41. (c) Franken, A.; Jalaie, M.; Dykstra, C. E. *Chem. Phys. Lett.* **1992**, *198*, 59. (d) Tsai, C. J.; Jordan, K. D. *Chem. Phys. Lett.* **1993**, *213*, 181. (e) Xantheas, S. S.; Dunning, T. H. *J. Chem. Phys.* **1993**, *98*, 8037. (f) Mhin, B. J.; Kim, J.; Lee, S.; Lee, J. Y.; Kim, K. S. *J. Chem. Phys.* **1994**, *100*, 4484. (g) Kim, J.; Mhin, B. J.; Lee, S. J.; Kim, K. S. *Chem. Phys. Lett.* **1994**, *219*, 243. (h) Pedulla, J. M.; Vila, F.; Jordan, K. D. *J. Chem. Phys.* **1996**, *105*, 11091. (i) Fowler, J. E.; Schaefer, III, H. F. *J. Am. Chem. Soc.* **1995**, *117*, 446.

(13) (a) Buck, U.; Huisken, F. *Chem. Rev.* **2000**, *100*, 3863. (b) Kim, J.; Kim, K. S. *J. Chem. Phys.* **1998**, *109*, 5886. (c) Ojamae, L.; Shavitt, I.; Singer, S. J. *J. Chem. Phys.* **1998**, *109*, 5547. (d) Sadlej, J.; Buch, V.; Kazimirski, J. K.; Buck, U. *J. Phys. Chem.* **1999**, *103*, 4933. (e) Lee, H. M.; Suh, S. B.; Lee, J. Y.; Tarakeshwar, P.; Kim, K. S. *J. Chem. Phys.* **2000**, *112*, 9759. (f) Xantheas, S. S. *Chem. Phys.* **2000**, *258*, 225. (g) Lee, H. M.; Suh, S. B.; Kim, K. S. *J. Chem. Phys.* **2001**, *114*, 10749. (h) Fanourgakis, G. S.; Apra, E.; Xantheas, S. S. *J. Chem. Phys.* **2004**, *121*, 2655. (i) Steinbach, C.; Andersson, P.; Melzer, M.; Kazimirski, J. K.; Buck, U.; Buch, V. *Phys. Chem. Chem. Phys.* **2004**, *6*, 3320. (j) Lenz, A.; Ojamae, L. *J. Phys. Chem.* **2006**, *110*, 13388.

(14) (a) Hammer, N. I.; Shin, J. W.; Headrick, J. M.; Diken, E. G.; Roscioli, J. R.; Weddle, G. H.; Johnson, M. A. *Science* **2004**, *306*, 675. (b) Paik, D. H.; Lee, I. R.; Yang, D. S.; Baskin, J. S.; Zewail, A. H. *Science* **2004**, *306*, 672. (c) Verlet, J. R. R.; Bragg, A. E.; Kammrath, A.; Cheshnovsky, O.; Neumark, D. M. *Science* **2005**, *307*, 5706. (d) Hammer, N. I.; Roscioli, J. R.; Johnson, M. A. *J. Phys. Chem. A* **2005**, *109*, 7896.

(15) (a) Lee, H. M.; Suh, S. B.; Tarakeshwar, P.; Kim, K. S. *J. Chem. Phys.* **2005**, *122*, 044309. (b) Lee, H. M.; Lee, S.; Kim, K. S. *J. Chem. Phys.* **2003**, *119*, 187. (c) Lee, H. M.; Kim, K. S. *J. Chem. Phys.* **2002**, *117*, 706. (d) Suh, S. B.; Lee, H. M.; Kim, J.; Lee, J. Y.; Kim, K. S. *J. Chem. Phys.* **2000**, *113*, 5273. (e) Kim, K. S.; Tarakeshwar, P.; Lee, J. Y. *Chem. Rev.* **2000**, *100*, 4145. (f) Jordan, K. D.; Wang, F. *Annu. Rev. Phys. Chem.* **2003**, *54*, 367.

(16) (a) Lisy, J. M. *Int. Rev. Phys. Chem.* **1997**, *16*, 267. (b) Vaden, T. D.; Forinash, B.; Lisy, J. M. *J. Chem. Phys.* **2002**, *117*, 4628. (c) Kim, J.; Lee, S.; Cho, S. J.; Mhin, B. J.; Kim, K. S. *J. Chem. Phys.* **1995**, *102*, 839. (d) Lee, H. M.; Kim, J.; Lee, S.; Mhin, B. J.; Kim, K. S. *J. Chem. Phys.* **1999**, *111*, 3995. (e) Kolaski, M.; Lee, H. M.; Choi, Y. C.; Kim, K. S.; Tarakeshwar, P.; Miller, D. J.; Lisy, J. M. *J. Chem. Phys.* **2007**, *126*, 074302.

(17) (a) Li, Z.; Scheraga, H. A. *Proc. Natl. Acad. Sci. U.S.A.* **1987**, *84*, 6611. (b) Day, P. N.; Pachter, R.; Gordon, M. S.; Merrill, G. N. *J. Chem. Phys.* **2000**, *12*, 2063.

(18) Elstner, M.; Porezag, D.; Jungnickel, G.; Elsner, J.; Haugk, M.; Frauenheim, T.; Suhai, S.; Seifert, G. *Phys. Rev. B* **1998**, *58*, 7260.

(19) Frisch, M. J.; Trucks, G. W.; Schlegel, H. B.; Scuseria, G. E.; Robb, M. A.; Cheeseman, J. R.; Montgomery, J. A., Jr.; Vreven, T.; Kudin, K. N.; Burant, J. C.; Millam, J. M.; Iyengar, S. S.; Tomasi, J. J.; Barone, V.; Mennucci, B.; Cossi, M.; Scalmani, G.; Rega, N.; Petersson, G. A.; Nakatsuji, H.; Hada, M.; Ehara, M.; Toyota, K.; Fukuda, R.; Hasegawa, J.; Ishida, M.; Nakajima, T.; Honda, Y.; Kitao, O.; Nakai, H.; Klene, M.; Li, X.; Knox, J. E.; Hratchian, H. P.; Cross, J. B.; Adamo, C.; Jaramillo, J.; Gomperts, R.; Stratmann, R. E.; Yazyev, O.; Austin, A. J.; Cammi, R.; Pomelli, C.; Ochterski, J. W.; Ayala, P. Y.; Morokuma, K.; Voth, A.; Salvador, P.; Dannenberg, J. J.; Zakrzewski, V. G.; Dapprich, S.; Daniels, A. D.; Strain, M. C.; Farkas, O.; Malick, D. K.; Rabuck, A. D.; Raghavachari, K.; Foresman, J. B.; Ortiz, J. V.; Cui, Q.; Baboul, A. G.; Clifford, S.; Cioslowski, J.; Stefanov, B. B.; Liu, G.; Liashenko, A.; Piskorz, P.; Komaromi, I.; Martin, R. L.; Fox, D. J.; Keith, T.; Al-Laham, M. A.; Peng, C. Y.; Nanayakkara, A.; Challacombe, M.; Gill, P. M. W.; Johnson, B.; Chen, W.; Wong, M. W.; Gonzalez, C.; Pople, J. A. *Gaussian 03*, revision A.1; Gaussian, Inc.: Pittsburgh, PA, 2003.

(20) (a) Becke, A. D. *J. Chem. Phys.* **1993**, *98*, 5648. (b) Lee, C.; Yang, W.; Parr, R. G. *Phys. Rev. B* **1988**, *37*, 785.

(21) (a) Helgaker, T.; Ruden, T. A.; Jorgensen, P.; Olsen, J.; Klopper, W. J. *Phys. Org. Chem.* **2004**, *17*, 913. (b) Helgaker, T.; Klopper, W.; Koch, H.; Noga, J. *J. Chem. Phys.* **1997**, *106*, 9639–9646.

(22) (a) Min, S. K.; Lee, E. C.; Lee, H. M.; Kim, D. Y.; Kim, D.; Kim, K. S. *J. Comput. Chem.* **2008**, *29*, 1208. (b) Lee, E. C.; Kim, D.; Jurečka, P.; Tarakeshwar, P.; Hobza, P.; Kim, K. S. *J. Phys. Chem. A* **2007**, *111*, 3446.

(23) (a) Császár, A. G.; Allen, W. D.; Schaefer, H. F., III *J. Chem. Phys.* **1998**, *108*, 9751. (b) Sinnokrot, M. O.; Sherrill, C. D. *J. Phys. Chem. A* **2004**, *108*, 10200.

(24) Lee, S. J.; Chung, H. Y.; Kim, K. S. *Bull. Korean Chem. Soc.* **2004**, *25*, 1061.

(25) (a) Benedict, W. S.; Gailar, G.; Plyler, E. K. *J. Chem. Phys.* **1956**, *24*, 1139. (b) Fraley, P. E.; Rao, K. N. *J. Mol. Spectrosc.* **1969**, *29*, 348.

(26) *CPMD*; Copyright IBM Corp., 1990−2001; Copyright MPI für Festkörperforschung Stuttgart, 1997−2001.

(27) Trouiller, N.; Martins, J. L. *Phys. Rev. B: Condens. Matter* **1991**, *43*, 1993.

(28) Grossman, J. C.; Schwegler, E.; Draeger, E. W.; Gygi, F.; Galli, G. *J. Chem. Phys.* **2004**, *120*, 300.

(29) Ziff, B. *Comput. Phys.* **1998**, *12*, 385.

(30) Schmitt, U. W.; Voth, G. A. *J. Chem. Phys.* **1999**, *111*, 9361.

(31) (a) Karthikeyan, S.; Singh, J. N.; Park, M.; Kumar, R.; Kim, K. S. *J. Chem. Phys.* **2008**, *128*, 244304. (b) Karthikeyan, S. ; Singh, J. N.; Kim, K. S. *J. Phys. Chem. A* **2008**, *112*, 6527.

(32) Pak, C.; Lee, H. M.; Kim, J. C.; Kim, D.; Kim, K. S. *Struct. Chem.* **2005**, *16*, 187.

JP804806U